

Thermal non-equilibrium effects in quantum reflection

Viola Druzhinina¹, Marcel Mudrich¹, Florian Arnecke², Javier Madroño^{2,3}, and Andreas Buchleitner¹

¹*Physikalisches Institut, Albert-Ludwigs Universität Freiburg, D-79104 Freiburg, Germany*

²*Physik Department, Technische Universität München, D-85747 Garching, Germany and*

³*Laboratoire de Physique Atomique, Moléculaire et Optique (unité PAMO), Université Catholique de Louvain, 2, chemin du Cyclotron, B-1348 Louvain-la-Neuve, Belgium*

(Dated: October 30, 2018)

We show that the quantum reflection coefficient of ultracold heavy atoms scattering off a dielectric surface can be tuned in a wide range by suitable choice of surface and environment temperatures. This effect results from a temperature dependent long-range repulsive part of the van der Waals-Casimir-Polder-Lifshitz atom-surface interaction potential.

PACS numbers: 34.50.-s; 34.35.+a; 31.30.jh; 42.50.Nn

The reflection of a matter wave from an attractive atom-surface interaction potential without reaching the classical turning point is known as quantum reflection (QR) [1]. The reflection probability approaches unity for vanishing primary kinetic (injection) energy of the atom, and can be enhanced by reducing the strength of the interaction potential. Furthermore, in thermal equilibrium light atoms are quantum reflected much more efficiently than heavy ones. These conditions have previously been realized in experiments in which neutral helium or hydrogen atoms were scattered off the surface of liquid helium [2, 3]. Later, neutral atoms prepared in the ground or in metastable states were reflected from a solid surface at grazing incidence [4, 5].

Rapid progress in laser cooling techniques, but also in surface preparation on the nanometer-scale, has made it possible to evidence low-velocity QR of Bose condensed sodium atoms at normal incidence with probabilities reaching 67%, possibly limited by mean-field interactions of the Bose-Einstein condensate (BEC) [6, 7]. Such high values could only be achieved using a nanostructured silicon surface with effectively reduced surface density, thereby lowering the interaction potential. Tunable atom-surface interactions, using evanescent waves created by a laser beam to enhance QR, have also been studied [8, 9]. High reflection probabilities open the possibility to utilize QR for trapping purposes [10].

In this Letter we present a new approach to controlling QR by exploiting thermal effects on the fundamental atom-surface interaction. We study QR of an atom from the surface of a dielectric solid body at thermal non-equilibrium. The Lifshitz force, which accounts for thermal fluctuations of the electromagnetic (EM) field, was found to add either attractively or repulsively to the long-range Casimir-Polder (CP) force, depending on whether the temperature of the substrate is higher or lower than that of the environment [11]. This either leads to suppressed or to enhanced QR, respectively. Thus, a QR coefficient close to unity may be expected even for heavy rubidium ⁸⁷Rb atoms at nano-Kelvin temperatures, scattering off an unstructured silicon (Si) surface,

provided the environment is approximately 1000 K hotter than the Si substrate. The detailed understanding of temperature effects in QR is of considerable importance, not only from a fundamental point of view, but also in the context of experimental realizations, such as storage of ultracold atoms on miniaturized atom-optical devices ('atom-chips') [12].

Let us start with an analysis of the force acting on a neutral atom near the surface of a dielectric body. It is caused by the interaction of the atom with the evanescent component of the thermal EM radiation field emitted by the body at temperature T_S . Additionally, the thermal blackbody radiation field reflected from the surface forms an intensity gradient causing a repulsive force acting between the atom and the surface [11, 13]. The temperature of the thermal blackbody radiation (*e. g.*, from the vacuum chamber) defines the environment temperature and is denoted as T_E . All expressions for the interaction potentials employed in this Letter are valid as long as T_E and T_S stay well below the lowest electronic transition energy of the atom, which is of the order of $k_B \times 10^4 \dots 10^5$ K, such that absorption of thermal photons is suppressed.

For thermal equilibrium ($T_E = T_S = T$), the atom-surface interaction potential was calculated using the theory of thermal fluctuations [14], and can generally be expressed by [15]

$$U_{\text{th}}^{\text{eq}}(r, T) = -\frac{k_B T \alpha_0}{4r^3} \frac{\varepsilon_0 - 1}{\varepsilon_0 + 1} G\left(\frac{r}{\lambda_T}\right). \quad (1)$$

Here, k_B , $\lambda_T = \hbar c / (k_B T)$ ($7.6 \mu\text{m}$ at 300 K), $\alpha_0 \equiv \alpha(0)$ and $\varepsilon_0 \equiv \varepsilon(0)$ denote Boltzmann's constant, the thermal photon wavelength, the static polarizability of the atom and the static dielectric permittivity of the surface, respectively. The function $G(r/\lambda_T)$ in Eq. (1), which interpolates between the two asymptotic regions $r \ll \lambda_T$ and $r \gg \lambda_T$, is explicitly defined in Ref. [15].

For $r \ll \lambda_T$, G tends towards $3\phi(\varepsilon_0)\lambda_T(\varepsilon_0 + 1)/2\pi r(\varepsilon_0 - 1)$. The potential Eq. (1) then adopts the well-known, temperature-independent CP form $U_{\text{th}}^{\text{eq}}(r) = -C_4/r^4$, with potential strength $C_4 = 3\alpha_0 \hbar c \phi(\varepsilon_0) / 8\pi$ [16], where the function $\phi(\varepsilon_0)$ describes

the dielectric properties of the surface, and is defined in Ref. [17]. This potential is caused by vacuum fluctuations of the EM field and is dominant at distances $l \ll r \ll \lambda_T$, where $l = \lambda_{tr}/2\pi$ is the effective wavelength of electronic transitions of the atom. For $r \ll l \ll \lambda_T$, however, the non-retarded van der Waals (vdW) potential is dominant, which needs to be incorporated. With the substitution $r/\lambda_T \rightarrow (r+l)/\lambda_T$ in function G , the potential Eq. (1) approaches at $r \ll \lambda_T$ the general van der Waals-Casimir-Polder (vdWCP) form $-C_4 r^{-3}/(r+l)$ [4, 18], which includes both non-retarded vdW and retarded CP potentials.

In the opposite case, when $r \gg \lambda_T$, G approaches unity, and the potential takes the form of the classical, temperature dependent Lifshitz potential, $U_{\text{th}}^{\text{eq}}(r, T) = -C_3(T)/r^3$, with strength $C_3(T) = \alpha_0 k_B T(\epsilon_0 - 1)/4(\epsilon_0 + 1)$. The Lifshitz potential has its origin in the thermal fluctuations of the EM field at finite temperature T [14].

If the system is out of thermal equilibrium, surface temperature T_S and environment temperature T_E differ from each other. $C_3(T)$ then turns into a function of T_E , and the Lifshitz potential acquires an additional term [11, 19],

$$U_{\text{th}}^{\text{neq}}(r, T_S, T_E) = -\frac{4\hbar\alpha_0}{\pi c^4(\epsilon_0 - 1)} \int_r^\infty dr' \int_0^\infty d\omega \times \\ \times \int_0^{\sqrt{\epsilon_0 - 1}} dt \omega^4 e^{-2r'\omega t/c} \left[\frac{1}{e^{\frac{\omega\lambda_{T_S}}{c}} - 1} - \frac{1}{e^{\frac{\omega\lambda_{T_E}}{c}} - 1} \right] \times \\ \times t^2 \sqrt{\epsilon_0 - 1 - t^2} \left[1 + \frac{\epsilon_0(2t^2 + 1)}{1 + t^2(\epsilon_0 + 1)} \right]. \quad (2)$$

For distances $r \gg l$, we derived Eq. (2) from the atom-surface force given in Ref. [11]. At distances closer to the surface thermal fluctuations play no role, and $U_{\text{th}}^{\text{neq}}$ is negligible compared to the vdWCP potential. Asymptotically, for $r \gg \lambda_{T_S}/\sqrt{\epsilon_0 - 1}$ and $r \gg \lambda_{T_E}/\sqrt{\epsilon_0 - 1}$, the quantum mechanical $U_{\text{th}}^{\text{neq}}(r, T_S, T_E)$ behaves like $C_2(T_S, T_E)/r^2$ with potential strength $C_2(T_S, T_E) = \pi\alpha_0 k_B^2 (T_E^2 - T_S^2)(\epsilon_0 + 1)/(12\hbar c\sqrt{\epsilon_0 - 1})$ [11]. In this limit, $U_{\text{th}}^{\text{neq}}(r, T_S, T_E)$ dominates the Lifshitz equilibrium potential $U_{\text{th}}^{\text{eq}}(r \gg \lambda_{T_E}, T_E) \simeq -C_3(T_E)/r^3$, and therefore determines the asymptotic behavior of the full atom-dielectric surface interaction potential,

$$U_{\text{th}}(r, T_S, T_E) = U_{\text{th}}^{\text{eq}}(r, T_E) + U_{\text{th}}^{\text{neq}}(r, T_S, T_E) \quad (3) \\ \rightarrow \frac{C_2(T_S, T_E)}{r^2}, \quad r \gg \left(\frac{\lambda_{T_S}}{\sqrt{\epsilon_0 - 1}}, \frac{\lambda_{T_E}}{\sqrt{\epsilon_0 - 1}} \right). \quad (4)$$

An enhanced attractive potential at non-equilibrium with $T_S > T_E = 310$ K was experimentally confirmed in [13], for a ^{87}Rb BEC placed 6...11 μm away from a fused-silica dielectric surface. In the case $T_E > T_S$, Eq. (4) leads to a repulsive barrier in the full atom-surface potential (Eq. (3)).

For ^{87}Rb atoms scattering off a Si surface ($\epsilon_0 \simeq 12$, $l \simeq 130$ nm, $C_4 \simeq 7.6 \times 10^{-37} \text{eV}/\text{m}^4$) at variable T_S

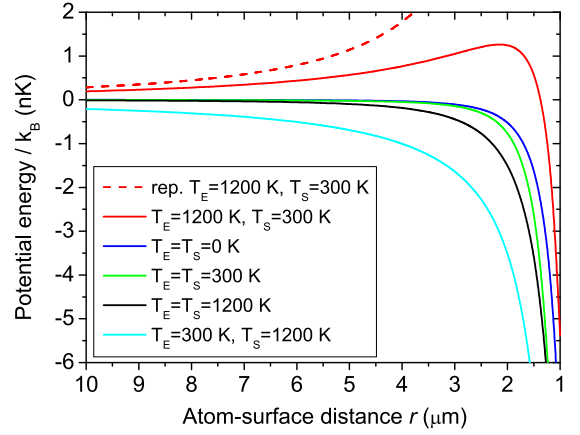


FIG. 1: (Color online) Numerical vdWCP-Lifshitz full potential energy (3), in units of temperature vs. distance between a ^{87}Rb atom and a Si surface, for different environment (T_E) and surface (T_S) temperatures: $T_E = 1200$ K, $T_S = 300$ K, $T_E = T_S = 0$ K, $T_E = T_S = 300$ K, and $T_E = 300$ K, $T_S = 1200$ K (solid lines from top to the bottom). The repulsive asymptote (Eq. (4)) is represented by the dashed line.

and T_E , the numerically evaluated interaction potential curves (Eq. (3)) are shown in Fig. 1. At thermal equilibrium the potential is attractive. The curves corresponding to different temperatures $T_E = T_S$ (second, third and fourth solid lines from bottom to the top) clearly differ from each other. In the non-equilibrium case of a hot surface, $T_S > T_E$, the potential is strongly attractive (lowest solid line) in the entire range of r . In contrast, a hot environment ($T_E = 1200$ K, $T_S = 300$ K) induces a repulsive potential barrier (upper solid line). The potential with the repulsive barrier coincides with its asymptote (4) (dashed line) at distances considerably larger than $\lambda_{T_E}/\sqrt{\epsilon_0 - 1} \simeq 0.6 \mu\text{m}$ and $\lambda_{T_S}/\sqrt{\epsilon_0 - 1} \simeq 2.3 \mu\text{m}$. A hot environment at $T_E = 1200$ K can easily be realized experimentally, *e. g.*, by means of heated plates mounted in the vicinity of the dielectricum.

Since QR sensitively depends on the shape and magnitude of the interaction potential, we may expect a considerable influence of temperature on the QR coefficient. In order to evaluate this effect, we simulate the QR coefficient numerically by matching two WKB-wave functions, valid very far from and very close to the surface, with the exact numerical solution of the Schrödinger equation, using the full numerical potential $U_{\text{th}}(r, T_S, T_E)$ as input [20]. Possible classical reflection from the short-range repulsive wall or sticking to the surface by inelastic scattering are not taken into account.

The numerically obtained QR coefficient of ^{87}Rb scattering off a Si surface as a function of the atomic injection velocity perpendicular to the surface, $v_i (= \hbar k_i/m)$ (bottom scale), for different choices of T_E and T_S are depicted in Fig. 2. Note the top scale $E_i/k_B = mv_i^2/(2k_B)$. The middle solid curve represents QR from the vdWCP interaction potential, without taking temperature effects into account. The lower solid curve shows $|R|^2$ for the system

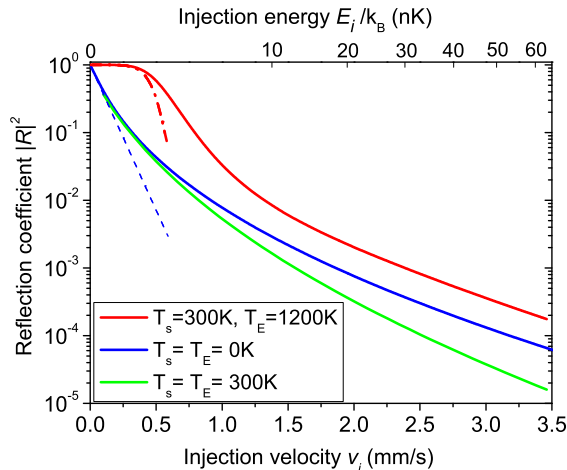


FIG. 2: (Color online) Numerical QR coefficient of ^{87}Rb from a Si surface, as a function of v_i (bottom scale) and E_i , in units of temperature (upper scale) for different T_E and T_S . The dashed and dash-dotted lines indicate the asymptotic behavior at low v_i given by Eq.'s (5) and (6) with $\gamma = 6.5$ and $b \simeq 2$ s/mm, respectively.

at room temperature ($T_S = T_E = 300$ K). Because of stronger attraction, the reflection probability is lowered. This might explain the measurement of smaller values of $|R|^2$ than the ones expected for single atom reflection [21]. The upper solid line in Fig. 2 displays QR evaluated using the full potential with a repulsive barrier with maximum $U_{\text{bar}} = U(r_{\text{bar}}, T_S, T_E) \simeq 1.26 \text{ nK} \times k_B$ located at the distance $r = r_{\text{bar}} \simeq 2 \mu\text{m}$. Clearly, $|R|^2$ is substantially increased. For $v_{i\text{bar}} = \sqrt{2U_{\text{bar}}/m} \simeq 0.49$ mm/s the atoms are $\simeq 65$ % reflected, as opposed to $|R|^2 \simeq 5$ % of this value in thermal equilibrium at room temperature. But also at injection energies exceeding the barrier height, at which pure quantum reflection takes place, the reflection coefficient exceeds the one at thermal equilibrium conditions at room temperature by at least one order of magnitude.

At zero-temperatures $T_E = T_S = 0$, and at very low values of v_i or C_4 , the QR coefficient adopts the well-known exponential form (dashed line in Fig. 2) [18]

$$|R|^2 \simeq \exp[-4k_i\beta_4] = \exp\left[-\frac{4m\beta_4}{\hbar}v_i\right], \quad k_i\beta_4 \ll 1. \quad (5)$$

Here, C_4 enters in terms of the length parameter $\beta_4 = (2mC_4/\hbar^2)^{1/2}$.

At non-equilibrium, for $v_i \rightarrow 0$, analysing the numerical results for $|R|^2$ reveals the exponential asymptote (dash-dotted line in Fig. 2)

$$|R|^2 \simeq \exp[-(bv_i)^\gamma]. \quad (6)$$

Our analytic investigations based on the theory developed in [22] allow us to define the parameter γ as $\gamma = \sqrt{1 + 4\beta_0}$. This parameter differs from unity if the system is out of thermal equilibrium through its dependence on $\beta_0 = 2mC_2(T_E, T_S)/\hbar^2$. Parameter b in Eq. (6) unfortunately cannot be represented by a simple analytic

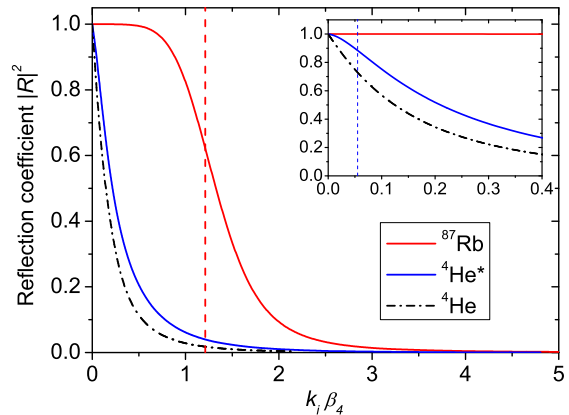


FIG. 3: (Color online) Numerical QR coefficient, as a function of the dimensionless parameter $k_i\beta_4$, for different atomic species scattering off a Si surface, at $T_E = 1200$ K and $T_S = 300$ K. Inset: Zooms into the region of small $k_i\beta_4$ -parameter. The vertical dashed lines denote the values of $(k_i\beta_4)_{\text{bar}}$, at which $E_i = U_{\text{bar}}$.

expression. The dash-dotted curve in Fig. 2 is obtained by fitting expression (6) to our numerical results in the region of small v_i with the fit parameter $b \simeq 2$ s/mm.

QR probabilities for various atomic species with strongly differing properties are best compared in terms of the dimensionless parameter $k_i\beta_4$. For this comparison we consider three different atomic species with pairwise similar m or α_0 — ^{87}Rb , $^4\text{He}^*$ in the metastable triplet state, and ground state ^4He — scattering off the same Si surface. Temperatures are held fixed at $T_E = 1200$ K and $T_S = 300$ K. The numerically obtained reflection coefficients are displayed in Fig. 3. Given the atomic species and temperatures, the parameter γ , which determines the asymptotic behavior, amounts to 6.5 (^{87}Rb : upper solid line), 1.7 ($^4\text{He}^*$: lower solid line) and 1.004 (^4He : dash-dotted line). The inset zooms into the same data at small values of $k_i\beta_4$. At injection energies equal to the height of the repulsive barrier, $k_i\beta_4$ has values $(k_i\beta_4)_{\text{bar}} = 1.21, 0.055, \text{ and } 2.4 \times 10^{-4}$, for Rb, He*, and He, respectively. For Rb and He*, the values for $(k_i\beta_4)_{\text{bar}}$ are depicted as vertical dashed lines in Fig. 3 and in its inset, respectively. They delimit the region of pure above-barrier reflection, $E_i > U_{\text{bar}}$, from the one where matter waves are reflected from the classical turning point, $E_i < U_{\text{bar}}$. For classical particles, $|R|^2(k_i\beta_4)$ would exhibit a Heavyside step function at $(k_i\beta_4)_{\text{bar}}$. The S-shaped behavior of $|R|^2$ highlights the quantum nature of the reflection process from a potential with a repulsive barrier. This behavior is modified by tunneling ($k_i\beta_4 < (k_i\beta_4)_{\text{bar}}$), and by above-barrier reflection ($k_i\beta_4 > (k_i\beta_4)_{\text{bar}}$), respectively.

Since ^{87}Rb and He^* have similar static polarizabilities ($\alpha_0 = 47.25 \text{ \AA}^3$ for ^{87}Rb , and 46.8 \AA^3 for $^4\text{He}^*$), their atom-surface potentials nearly coincide, with barrier heights corresponding to a temperature $T_{\text{bar}} = \hbar^2(k_i\beta_4)_{\text{bar}}^2/(2mk_B\beta_4^2) \simeq 1.26$ nK. Fig. 3 shows, however, that the QR coefficients at $k_i\beta_4 = (k_i\beta_4)_{\text{bar}}$ (the intersec-

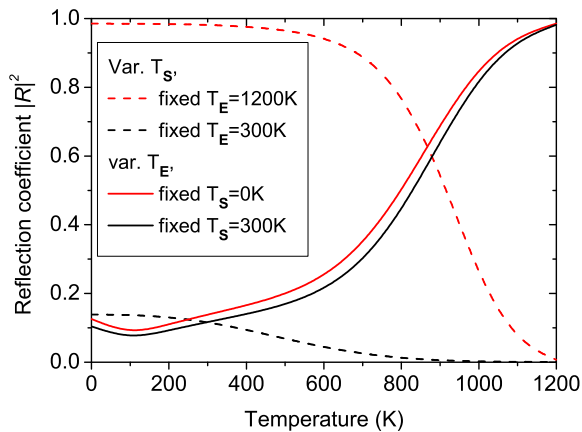


FIG. 4: (Color online) Numerical QR coefficient of ^{87}Rb atoms scattering off a Si surface, as a function of environment or surface temperature, with the other one fixed. Upper and lower dashed lines: Dependence on T_S , at fixed $T_E = 1200$ K and $T_E = 300$ K, respectively. Upper and lower solid lines: Dependence on T_E , at fixed $T_S = 0$ K and $T_S = 300$ K, respectively. $k_i\beta_4$ was set to 0.68.

tions of dashed lines with solid ones) are quite different for these two species. At the same fixed E_i , light atoms are reflected much more efficiently than heavy ones. This mass dependence is a typical feature, which also applies to above-barrier reflection from a pure attractive potential. Without a repulsive barrier, the upper solid curve (^{87}Rb) would be shifted to even smaller values of $k_i\beta_4$ than the dash-dotted one (^4He , $\alpha_0 = 0.205 \text{ \AA}^3$). In contrast, in the presence of a barrier, $|R|^2$ increases significantly for heavy ^{87}Rb . Furthermore, for ^4He and $^4\text{He}^*$ having same m but different α_0 , the QR coefficients have different magnitudes at small fixed value of $k_i\beta_4$, due to different values of γ .

In order to illustrate the potential to control QR efficiency by adjusting the system temperatures, Fig. 4 shows the dependence of $|R|^2$ on either T_E or T_S , with the other one fixed, for the $^{87}\text{Rb}/\text{Si}$ system. We choose $k_i\beta_4 = 0.68$, which corresponds to $E_i \simeq 0.4 \text{ nK} \times k_B$. At $T_S = T_E$ all curves in Fig. 4 have very small but distinct values, due to above-barrier reflection from the attractive potential in thermal equilibrium at different temperatures. At T_E between 0 and 200 K the solid curves reveal the competition between $U_{\text{th}}^{\text{eq}}(r, T_E)$ and $U_{\text{th}}^{\text{neq}}(r, T_S, T_E)$. As T_S falls below the fixed value of T_E (dashed curves) or T_E rises above the fixed value of T_S (solid curves), a repulsive barrier emerges in the atom-surface potential. Consequently, the QR coefficient grows nearly to unity, except for the T_S -dependence at $T_E = 300$ K, at which the barrier height remains very low. Clearly, heating the environment to a temperature which is by up to 900 K higher than the one of the surface, drastically enhances the QR probability in the entire temperature range, as opposed to a weak increase of $|R|^2$ when just cooling the

surface close to 0 K.

In conclusion, we have shown that the QR probability is significantly enhanced in the presence of a repulsive barrier in the atom-surface interaction potential, which emerges when the environment temperature exceeds the one of the surface. By changing one of the temperatures it is possible to vary the QR probability in a wide range, in particular when using heavy atoms. In analogy to a macroscopic sphere near a surface [23], a heavy ultracold atom could be quantum levitated a few micrometers above a surface. This opens new perspectives for guiding and trapping ultracold atoms on surfaces, *e.g.* on atom chips.

Helpful discussions with M. Antezza, H. Friedrich and T. Wellens are acknowledged. We are grateful to the Schlieben-Lange-Program fellowship for supporting the work of V.D.

-
- [1] V. L. Pokrovskii, S. K. Savvinykh, and F. K. Ulinich, *Sov. Phys. JETP* **34**, 879(1119) (1958).
 - [2] V. U. Nayak, D. O. Edwards, and N. Masuhara, *Phys. Rev. Lett.* **50**, 990 (1983).
 - [3] J. J. Berkhout *et al.*, *Phys. Rev. Lett.* **63**, 1689 (1989).
 - [4] F. Shimizu, *Phys. Rev. Lett.* **86**, 987 (2001).
 - [5] V. Druzhinina and M. DeKieviet, *Phys. Rev. Lett.* **91**, 193202 (2003).
 - [6] T. A. Pasquini *et al.*, *Phys. Rev. Lett.* **95**, 113202 (2005).
 - [7] R. G. Scott *et al.*, *Phys. Rev. Lett.* **95**, 073201 (2005).
 - [8] R. Côté, B. Segev, and M. G. Raizen, *Phys. Rev. A* **58**, 3999 (1998).
 - [9] A. Langragin *et al.*, *Phys. Rev. Lett.* **77**, 1464 (1996).
 - [10] A. Jurisch and H. Friedrich, *Phys. Lett. A* **349**, 230 (2006), J. Madroñero and H. Friedrich, *Phys. Rev. A* **75**, 022902 (2007)
 - [11] M. Antezza, L. P. Pitaevskii, and S. Stringari, *Phys. Rev. Lett.* **95**, 113202 (2005).
 - [12] R. Folman *et al.*, *Adv. At. Mol. Opt. Phys.* **48**, 263 (2002).
 - [13] J. M. Obrecht *et al.*, *Phys. Rev. Lett.* **98**, 063201 (2007).
 - [14] E. M. Lifshitz, *Dokl. Akad. Nauk SSSR* **100**, 879 (1955).
 - [15] M. Antezza, L. P. Pitaevskii, and S. Stringari, *Phys. Rev. A* **70**, 053619 (2004).
 - [16] H. B. G. Casimir and D. Polder, *Phys. Rev.* **73**, 360 (1948).
 - [17] I. E. Dzyaloshinskii, E. M. Lifshitz, and L. P. Pitaevskii, *Adv. Phys.* **10**, 165 (1961).
 - [18] H. Friedrich, G. Jacoby, and C. G. Meister, *Phys. Rev. A* **65**, 032902 (2002).
 - [19] C. Henkel *et al.*, *J. Opt. A: Pure Appl. Opt.* **4**, S109 (2002).
 - [20] R. Côté, H. Friedrich, and J. Trost, *Phys. Rev. A* **56**, 1781 (1997).
 - [21] T. A. Pasquini *et al.*, *Phys. Rev. Lett.* **93**, 223201 (2004).
 - [22] F. Arnecke, H. Friedrich, and P. Raab, *Phys. Rev. A* **78**, 052711 (2008).
 - [23] J. N. Munday, F. Capasso, and V. A. Parsegian, *Nature* **457**, 170 (2009).